Journal of Hazardous Materials 203–204 (2012) 213–220

Contents lists available at SciVerse ScienceDirect

Journal of Hazardous Materials

journal homepage: www.elsevier.com/locate/jhazmat

The synthesis of poly(vinylphosphonic acid-*co*-methacrylic acid) microbeads by suspension polymerization and the characterization of their indium adsorption properties

Noh-Seok Kwak, Youngmin Baek, Taek Sung Hwang*

Department of Applied Chemistry and Biological Engineering, Chungnam National University, 79 Daehangno, Yuseong-gu, Daejeon 305-764, Republic of Korea

ARTICLE INFO

Article history:
Received 1 September 2011
Received in revised form
16 November 2011
Accepted 2 December 2011
Available online 14 December 2011

Keywords:
Suspension polymerization
Ion exchange
Microbeads
Indium adsorption

ABSTRACT

Poly(vinylphosphonic acid-*co*-methacrylic acid) microbeads were synthesized by suspension polymerization, and their indium adsorption properties were investigated. The obtained microbeads were characterized by Fourier transform infrared (FT-IR) spectroscopy and scanning electron microscopy (SEM). The microbeads were wrinkled spheres, irrespective of the components, and their sizes ranged from 100 to 200 μm. The microbeads were thermally stable up to 260 °C. As the vinylphosphonic acid (VPA) content was increased, the synthetic yields and ion-exchange capacities decreased and the water uptakes increased. The optimum synthetic yield, ion-exchange capacity and water uptake were obtained at a 0.5 mol ratio of VPA. In addition, the maximum adsorption predicted by the Langmuir adsorption isotherm model was greatest at a 0.5 mol ratio of VPA.

1. Introduction

Indium and its compounds have a wide range of industrial applications whose rapid development has increased their consumption [1]. However, indium is widely dispersed in nature and only typically found at low concentrations in some zinc, copper and lead sulfide ores. Therefore, the development of indium recovery technology is in demand. Furthermore, indium wastewater is suspected to be carcinogenic to humans, and it is known that indium and its compounds induce cytotoxicity in several animal experiments [2,3]. Hence, the interest in indium recovery is not only increasing in the field of rare metal recovery but also in that of heavy metal elimination.

Several studies on methods for indium recovery have been reported, including liquid–liquid extraction (LLE) [4], co-precipitation [5], solid-phase extraction [6], electroanalytical techniques [7,8] and ion exchange methods. The primary disadvantage of LLE is the loss of extractant into the aqueous phase, which may result in economic limitations and environmental hazards. The other indium recovery technologies also exhibit disadvantages, such as a high solvent-recovery cost, environmental and health hazards and time-consuming processing methods. Ion exchange methods are simpler than the other technologies and have the advantage of a low recovery cost.

A few investigations on metal recovery using ion exchange have been reported. Fortes et al. reported indium adsorption onto ion exchangers that contained different organic functional groups, such as iminodiacetic acid, diphosphonic acid and aminophosphonic acid [9]. Mendes and Martins reported the adsorption of nickel and cobalt onto some commercially available chelating ion-exchange resins [10]. However, most researchers involved in indium recovery using ion exchange have only reported its adsorption properties on commercially available ion exchange resins. In this study, microbeads were prepared as ion exchangers by suspension polymerization, and their adsorption properties were investigated.

Suspension polymerization has been widely used in industrial applications to produce specialty polymer particles, such as ion-exchange resins, chromatographic separation media and supports for enzyme immobilization. Suspension polymerization is a suitable polymerization technique for the production of large polymer beads, typically in the range of 5–1000 μm [11]. Numerous reports on the preparation of ion-exchange resins by suspension polymerization have appeared in the literature. Lin et al. reported the synthesis of *p*-(ω-sulfonic-perfluoroalkylated)polystyrene ion-exchange resin by suspension polymerization [12], and Coutinho et al. described the preparation of a pellicular ion-exchange resin [13].

In this study, the microbeads were synthesized by suspension polymerization using vinylphosphonic acid (VPA) and methacrylic

* Corresponding author. Tel.: +82 42 821 5687; fax: +82 42 822 8995.
E-mail address: tshwang@cnu.ac.kr (T.S. Hwang).

0304-3894/$ – see front matter © 2012 Elsevier B.V. All rights reserved.
doi:10.1016/j.jhazmat.2011.12.020

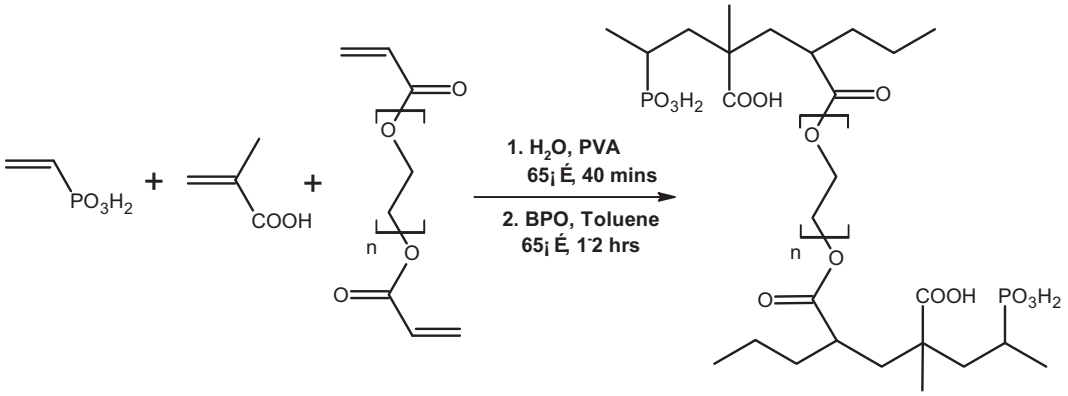

Fig. 1. A schematic mechanism for the synthesis of poly(vinylphosphonic acid-*co*-methacrylic acid).

acid (MAA) as monomers and poly(ethylene glycol) diacrylate (PEGDA) as a crosslinking agent. VPA has a chelate which allows exchanging In^{3+} and it is possible to synthesize by radical polymerization due to its vinyl group. However, VPA is very expensive and VPA alone make a synthesis yield decrease. On the contrary, MAA allows a yield to increase and furthermore its weak acid group, —COOH, helps ion-exchange capacity to increase. Therefore, in this study, the basic properties of ion exchange beads at a different VPA content were investigated. Furthermore, the adsorption properties and thermodynamic properties of the best condition's sample were examined. The structure and morphology of the microbeads were confirmed by Fourier transform infrared (FT-IR) spectroscopy and scanning electron microscopy (SEM).

2. Experiment

2.1. Materials

VPA (90%) and MAA (99.5%) (used as monomers) and PEGDA (M_w = 258) (used as the crosslinking agent) were obtained from Sigma–Aldrich Co. (New York, USA). Benzoyl peroxide (BPO, 75%) (used as an initiator) and poly(vinyl alcohol) (PVA) (used as a stabilizer) were purchased from Lancaster (Morecambe, England) and Junsei (Tokyo, Japan), respectively. 1-(2-Pyridylazo)-2-naphtol (PAN) and ethylene diamine tetraacetic acid (EDTA) (used as an indicator and as a titrant, respectively) were purchased from Sigma–Aldrich Co. (New York, USA) and Samchun Co. (Seoul, Korea), respectively. Twice-distilled water, toluene and ethanol were used as solvents.

2.2. Preparation of poly (VPA-co-MAA) ion-exchange microbeads

Different monomer ratios of poly(VPA-*co*-MAA) were synthesized by suspension polymerization. Fig. 1 shows the structures of the monomers and poly(VPA-*co*-MAA). The polymerization was conducted in a 500 mL three-neck round-bottom flask equipped with a mechanical stirrer (IKA® RW20 digital, IKA company, Osaka, Japan), a condenser, a nitrogen inlet, a thermometer and a dropping funnel. VPA, MAA and PEGDA were dissolved in a mixture of distilled water and PVA at 65 °C. The solution was placed under continuous strong agitation until all of the monomers were completely dissolved. BPO (as an initiator) and toluene were then added to the solution with a dropping funnel. The polymerization was performed in airtight equipment at 65 °C and maintained for 1–2 h with stirring (750 rpm). Table 1 shows the mole ratios of the syntheses.

The synthetic yield of the microbeads was determined by Eq. (1):

$$\text{Synthetic yield } (\%) = \frac{W_d}{W_m} \times 100 \quad (1)$$

where W_d is the weight of the clean and dry polymer beads (g), and W_m is the initial weight of the monomer (g).

2.3. The characterization of poly(vinylphosphonic acid-co-methacrylic acid)

The structures of the poly(VPA-*co*-MAA) samples were characterized using FT-IR (IR Prestige-21, Shimadzu, Kyoto, Japan). Discs containing 1 mg of sample and 150 mg of KBr were prepared on a press using a 60–70 kN compression force. The FT-IR spectra were collected over a wavenumber range of 4000–600 cm^{-1}; the resolution was 4 cm^{-1}, and 20 scans were taken.

The elemental analysis of poly(VPA-*co*-MAA) was performed with energy-dispersive X-ray spectroscopy (EDS, JSM-7000F, JEOL, Akishima, Japan), which was attached to the scanning electron microscope (SEM). Incident electron-beam energies from 0.5 to 30 keV were used. In all cases, the beam was at a normal incidence to the sample surface and the measurement time was 100 s. All of the surfaces of the samples were covered with osmium using the ion sputtering method.

The thermal decomposition behaviors of the microbeads were investigated using TGA (TA Instruments Q500, New Castle, DE, USA)

Table 1
Synthesis conditions of poly (vinylphosphonic acid-*co*-methacrylic acid).

Sample code	Monomer (mole ratio)		Crosslinking agent	Stabilizer	Initiator
	VPA	MAc	PEGDA	PVA	BPO
VMP00-3	0.00	1.00	30 wt%	0.01 wt%	0.01 wt%
VMP02-3	0.25	0.75			
VMP05-3	0.50	0.50			
VMP07-3	0.75	0.25			
VMP10-3	1.00	0.00			
VMP00-4	0.00	1.00	40 wt%		
VMP02-4	0.25	0.75			
VMP05-4	0.50	0.50			
VMP07-4	0.75	0.25			
VMP10-4	1.00	0.00			
VMP00-5	0.00	1.00	50 wt%		
VMP02-5	0.25	0.75			
VMP05-5	0.50	0.50			
VMP07-5	0.75	0.25			
VMP10-5	1.00	0.00			

in a range from 25 to 600 °C at a heating rate of 10 °C/min under a nitrogen atmosphere.

2.4. Water uptake and cation-exchange capacity

The dried sample was immersed in water for 24 h. The sample was removed from the water and wiped with absorbent paper to remove excess water adhered to the surface. The sample was then weighed on a balance. The water uptake was calculated by Eq. (2):

$$\text{Water uptake } (\%) = \frac{(W_w - W_d)}{W_d} \times 100 \quad (2)$$

where W_w and W_d are the weight of the sample under wet and dry conditions, respectively.

The ion-exchange capacity (IEC) of the sample was determined by the titration method. The sample was equilibrated in 100 mL of 0.1 N NaOH solution at room temperature for 24 h. The sample was then removed, and 20 mL of the NaOH solution was titrated with 0.1 mol/L HCl solution containing a drop of a phenolphthalein solution (0.1% in ethanol) as a pH indicator. The experimental IEC was calculated according to Eq. (3):

$$\text{IEC (meq/g)} = \frac{(W_{NaOH} \times C_{NaOH}) - (W_{HCl} \times C_{HCl})}{W_d} \quad (3)$$

where V_{NaOH} and V_{HCl} are the volume of the NaOH solution and the consumed volume of the HCl solution, respectively, and C_{NaOH} and C_{HCl} are the concentrations of NaOH and HCl, respectively [14,15].

2.5. Indium-adsorption properties

Isotherm experiments of indium adsorbed onto microbeads were performed at pH 8. The microbeads were mixed with an indium solution in a shaker operated at 200 rpm for 4 h at 25 °C to achieve equilibrium. The Langmuir and Freundlich equations were applied to the adsorption equilibria for the microbeads.

The indium adsorption properties were determined by the EDTA titration method [16]. A 0.1 g sample was immersed in a 100 mg/L indium solution, and a 40 mL aliquot was then collected from this solution. 1-(2-Pyridylazo)-2-naphtol (PAN) was used as an indicator. The amount of indium adsorption was calculated by equation (4):

$$\text{Amount of indium adsorption (mmol/g)} = \frac{(C_{in}V_{in} - C_{ETDA}V_{EDTA})}{W_{resin}} \quad (4)$$

where C_{in} and V_{in} are the mole concentration and volume of the initial indium solution, respectively, and C_{EDTA} and V_{ETDA} are the mole concentration and consumed volume of the EDTA solution, respectively.

3. Results and discussion

3.1. Preparation of poly(vinylphosphonic acid-co-methacrylic acid)

The synthetic yields of poly(VPA-*co*-MAA) are shown in Fig. 2. The maximum synthetic yield was 82% in the absence of VPA. The synthetic yields were dependent on the VPA content, and a decreasing trend in the yield was observed. However, the synthetic yield increased as the concentration of the crosslinking agent increased. According to Tuncel [17], the synthetic yield was affected by both the monomer/diluent ratio and the concentration of the crosslinking agent but not by the agitation rate, which was consistent with our results. In this study, the synthetic yield increased at higher concentrations of the crosslinking agent. However, the influence of the monomer ratio was greater than that of the crosslinking agent.

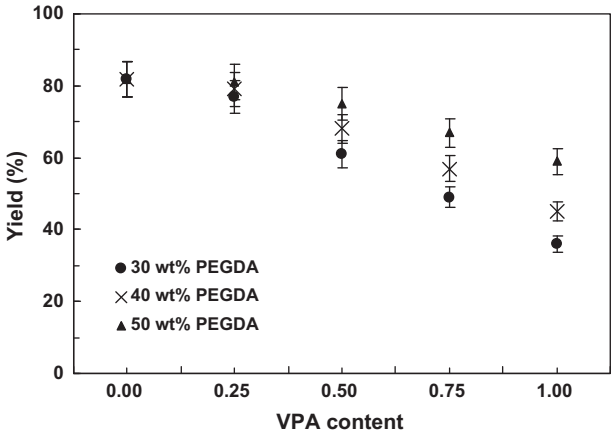

Fig. 2. The effect of the VPA content and crosslinking-agent concentration on the poly(VPA-*co*-MAA) yields.

This is confirmed by the differences in the synthetic yields for different VPA contents. At lower VPA concentrations, the change in the crosslinking agent contents affects the change in the MAA contents while at a higher VPA concentrations, the change in the crosslinking agent contents affects the change in the VPA contents. Therefore, the differences in the synthetic yields at higher VPA concentrations suggest that VPA had a large influence on yield. This trend indicates that the conversion of VPA radicals was lower than that of MAA and PEGDA. On the other hand, the microbeads were not formed at a crosslinking-agent concentration of 20 wt%.

3.2. Structure analysis

Fig. 3 shows the FT-IR spectrum of poly(vinylphosphonic acid-*co*-methacrylic acid). The broad band at approximately 3500 cm^{-1} was attributed to OH single vibrations. Bands resulting from methylene C—H stretching vibrations were observed at approximately 2941 cm^{-1}. A strong band at 1760 cm^{-1} resulted from C=O stretching vibrations in MMA, and the other band at 1740 cm^{-1} resulted from C=O stretching vibrations in PEGDA. In general, the intense C=O stretching vibration of an ester occurs at a shorter wavelength than that of a normal carboxylic acid [18]. Therefore, the peak at 1760 cm^{-1} decreased with increasing VPA concentration, which decreases the MMA concentration while the amount of PEGDA was fixed. The strong band at 1194 cm^{-1} was ascribed to the stretching vibrations of P=O, and the absorption band at 965 cm^{-1} was ascribed to the P—OH stretching band. The peaks at 1194 cm^{-1} and 965 cm^{-1} did not appeared in VMP00-3 and the peak intensities increased as the increase in the content of VPA [18,19]. The FT-IR results provided strong evidence that poly(vinylphosphonic acid-*co*-methacrylic acid) was successfully synthesized.

3.3. Thermal analysis

The thermal stability of the synthesized microbeads was established by TGA. Fig. 4 shows the TGA thermograms of the microbeads prepared with different concentrations of the crosslinking agent. Their first weight loss at approximately 100 °C resulted from moisture loss, and the second weight loss in the range of 260–400 °C was caused by the decomposition of —COOH and $-PO_3H_2$ in the branch. Therefore, the magnitude of the second weight loss decreased with increasing concentration of the crosslinking agent with a consequential decrease in the concentrations of the monomers. The third weight loss above 400 °C was caused by the decomposition of the polymer network. Hence, the microbeads synthesized in this study

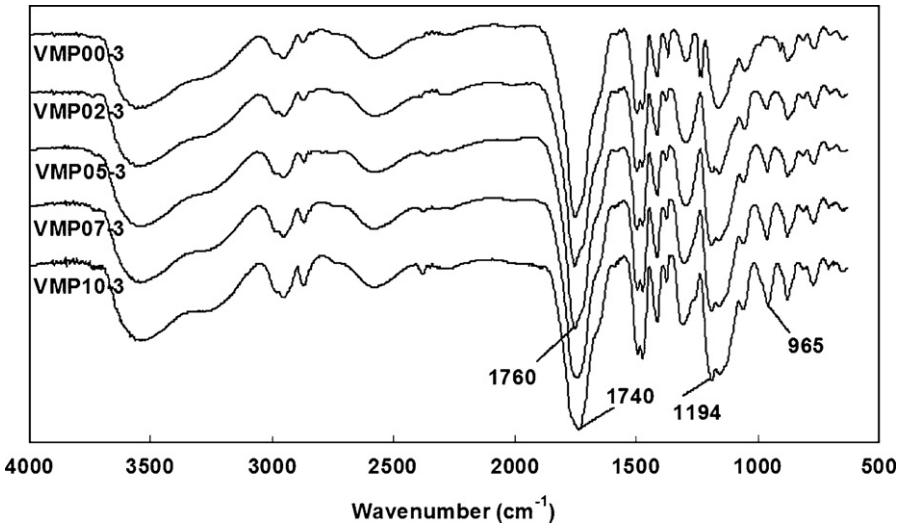

Fig. 3. FT-IR spectra of poly(vinylphosphonic acid-*co*-methacrylic acid) microbeads.

were thermally stable at temperatures up to 260 °C. The presence of VPA exhibited no effect on the observed weight loss.

3.4. SEM-EDS

For morphological evaluations, micrographs of the microbeads with different components were obtained and are presented in Fig. 5. The microbeads were wrinkled spheres, irrespective of the components, and their sizes ranged from 100 to 200 μm. No differences in the bead sizes were observed by varying the VPA content. In general, the particle size is directly proportional to the container diameter, the viscosity of the droplet phase, the ratio of the droplet phase to the suspension medium and the internal tension between the two immiscible phases. The particle size is inversely proportional to the stirrer diameter, the stirring rate, the viscosity of the suspension medium and the stabilizer concentration [20,21].

Table 2 shows the proportions of carbon, oxygen and phosphorous in the samples. The phosphorus content in the VMP02-3, VMP05-3, VMP07-3 and VMP10-3 samples was determined to be 1.00%, 1.96%, 2.68% and 3.76%, respectively, from the EDS data. Based on the monomers used in the polymerization, the phosphorous content should have been 4.10%, 7.96%, 11.60% and 15.04%, respectively. Therefore, the extent of the conversion of VPA radicals was lower than that of the other monomers. Similar results are shown in Section 3.1.

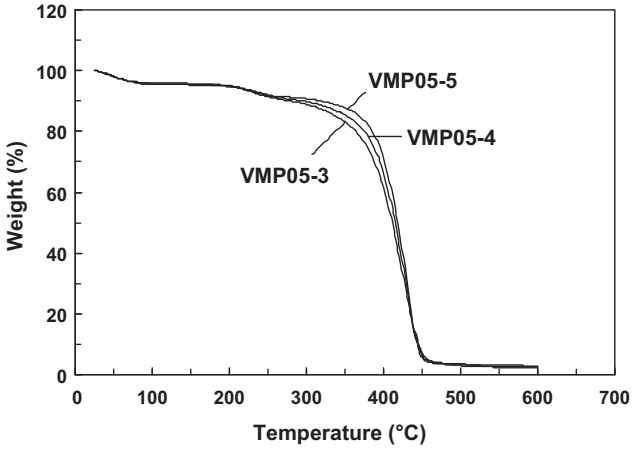

Fig. 4. TGA curves of the synthesized microbeads with different crosslinking-agent concentrations.

3.5. Ion-exchange capacity (IEC)

The IEC provides an indication of the acid group content in the microbeads. The experimental IEC values are given in Fig. 6. The IEC values increased as the VPA concentration decreased, which was accompanied by a consequential increase in MAA concentration. These results indicated that numerous sodium ions adsorbed onto the —COOH functional group rather than onto the $-PO_3H_2$ group and that the degree of conversion of VPA was lower than that of MAA and PEGDA. Similar results are shown in Fig. 2 and Table 2. However, the IEC decreased as the concentration of the crosslinking agent increased because the increasing amounts of crosslinking agent resulted in a corresponding decrease in the concentration of the monomers, which contain the functional groups.

3.6. Water uptake

Hydrophilicity and crosslinking ratios were the factors determined to affect the water uptake of the hydrophilic polymers [22]. The water uptake occurred when the microbeads were placed in an aqueous medium because the chemicals used in this study were hydrophilic. The water uptake values are given in Fig. 7. The water uptake was proportional to the VPA content inversely proportional

Table 2
Elemental analysis data obtained from EDS.

Sample code	Carbon (%)	Oxygen (%)	Phosphorus (%)
VMP00-3	60.12	39.88	0.00
VMP02-3	58.53	40.17	1.30
VMP05-3	57.53	40.51	1.96
VMP07-3	56.78	40.54	2.68
VMP10-3	55.33	40.91	3.76
VMP00-4	59.91	40.09	0.00
VMP02-4	58.70	40.22	1.08
VMP05-4	57.86	40.37	1.77
VMP07-4	56.89	40.55	2.56
VMP10-4	56.11	40.68	3.21
VMP00-5	60.14	39.86	0.00
VMP02-5	59.26	40.03	0.71
VMP05-5	58.35	40.32	1.33
VMP07-5	57.22	40.51	2.27
VMP10-5	56.30	40.73	2.97

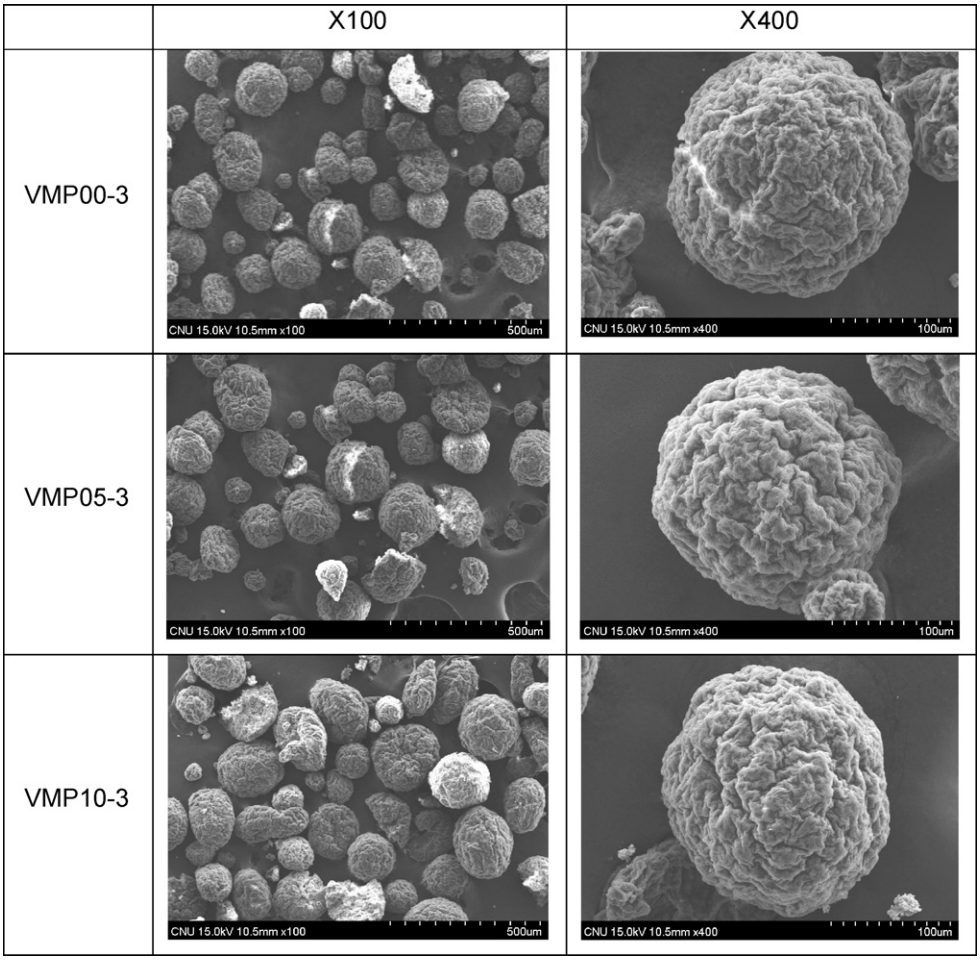

Fig. 5. SEM photographs of microbeads with different VPA contents.

to the amount of the crosslinking agent. This is because the water uptake is affected by hydrophilicity and the hydrophilicity of VPA is greater than that of MAA. Additionally, the increase in the concentration of crosslinking agent and the resultant increase in the crosslinking density prevent the water from accessing the inside of the microbeads. An increase in water uptake is an unavoidable result because an increase in IEC leads to an increase in water uptake, but too large an increase reduces the durability of the microbeads. Thus it is important to maintain a proper water uptake.

3.7. Indium adsorption isotherms

The adsorption of In (III) ions onto the synthesized microbeads is given in Fig. 8. As shown in Fig. 8, the indium adsorption is thought to be a chemisorption between the metal ion and three O^- in VPA and MAA by the chelate effect. To analyze adsorption behavior, the adsorption isotherms and thermodynamics were investigated.

The equilibrium adsorption isotherm indicates the interactions between the adsorbents and solutes when the adsorption process

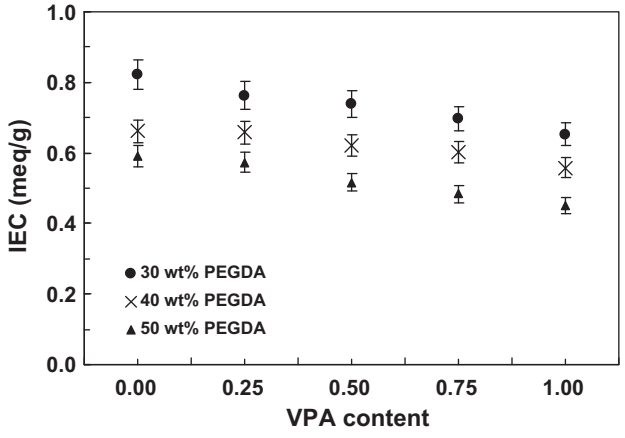

Fig. 6. The effect of VPA content and crosslinking-agent concentration on the ion-exchange capacity.

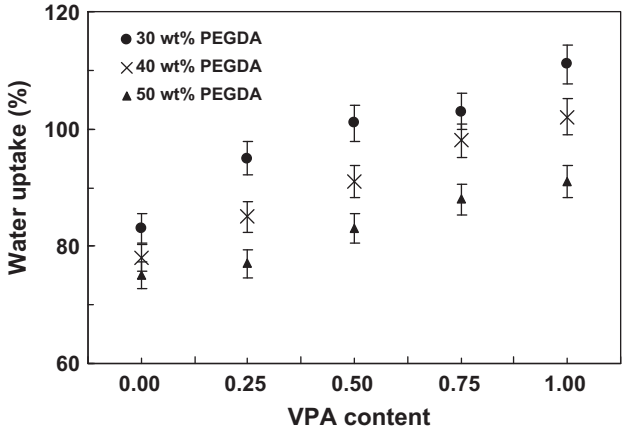

Fig. 7. The effect of VPA content and crosslinking-agent concentration on water uptake.

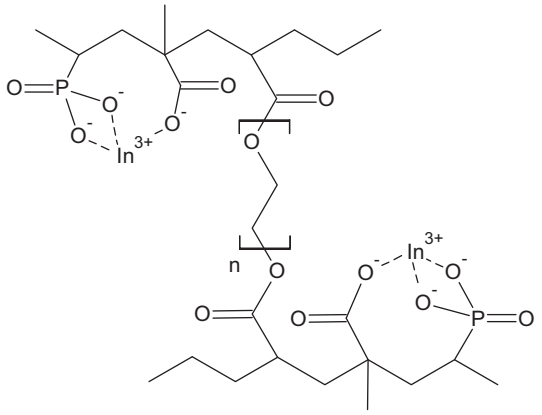

Fig. 8. An adsorption mechanism for adsorption of indium onto the microbeads.

reaches equilibrium. Isotherm experiments on the adsorption of indium onto microbeads are commonly fit to both the Langmuir and Freundlich models [23–27]:

$$\frac{C_e}{q_e} = \frac{1}{(K_L q_m)} + \frac{C_e}{q_m} \quad (5)$$

$$q_e = K_F C_e^{1/n} \quad (6)$$

where C_e is the equilibrium concentration (mmol/L), q_e is the adsorption capacity at equilibrium (mmol/g resin) and q_m is the maximum amount of solute exchanged per gram of microbeads (mmol/g resin); K_L and K_F are the Langmuir and Freundlich constants, respectively, which are related to the adsorption capacity, and n is a constant to be determined. A basic assumption of the Langmuir model is that the adsorption takes place at specific, homogeneous sites in the adsorbent; hence, it is confined to a mono-layer of adsorption whereas the Freundlich model deals with equilibrium on a heterogeneous surface where the adsorption energy is not homogeneous for all adsorption sites. Hence the Freundlich model can be applied to multi-layer adsorption.

The experimental adsorption isotherms of the microbeads are shown in Fig. 9 and all constants obtained from the experimental data in Fig. 9 are listed in Table 3. The Langmuir and Freundlich models calculated from the data in Table 3 are also illustrated in Fig. 9. The Langmuir constants, such as K_L and q_m, were obtained by the linear plot of C_e/q_e versus C_e from Eq. (5), and the Freundlich constants, such as K_F and n, were determined with the plot of log q_e versus log C_e from Eq. (6). As shown in Fig. 9, the experimental data corresponded better to the Langmuir model; therefore the adsorption behavior of indium onto the synthesized microbeads is considered to be the adsorption onto mono-layer.

Sample VMP05-3 exhibited the greatest adsorption. As the mole ratio of VPA increased, the number of $-PO_3H$ groups, which strongly affects indium adsorption, increased slightly. However, the number of −COOH groups decreased dramatically because of the VPA conversion and the synthetic yields. These results explain why the degree of indium adsorption decreased in samples VMP07-3 and VMP10-3 and are in accordance with the data in Table 3. The maximum value of q_m, the maximum amount of solute exchanged per gram of microbead, was attained at a 50% mol ratio of VPA.

Table 3
Isotherm constants for the adsorption of indium onto the microbeads.

Sample code	Langmuir model			Freundlich model		
	K_L	q_m	R^2	K_F	n	R^2
VMP00-3	4.69	0.53	0.997	0.41	3.23	0.945
VMP02-3	4.91	0.65	0.997	0.44	3.10	0.926
VMP05-3	5.24	0.70	0.998	0.49	3.07	0.966
VMP07-3	2.75	0.63	0.994	0.40	2.82	0.973
VMP10-3	3.72	0.47	0.995	0.33	3.39	0.977

Table 4
Thermodynamic parameters for indium ion adsorption onto VMP05-3.

Temperature (K)	ΔG° (kJ/mol)	ΔH° (kJ/mol)	ΔS° (J/mol K)
298.15	−6.9	−48.18	−138.84
308.15	−5.2		
318.15	−4.1		

3.8. Thermodynamics of indium adsorption

The thermodynamic parameters such as the standard Gibbs free energy (ΔG°), standard enthalpy change (ΔH°) and standard entropy change (ΔS°) must be considered to determine the spontaneity of the adsorption process [28–30]. These parameters can be calculated from the following Eqs. (7)–(9):

$$\Delta G^\circ = -RT \ln K^\circ \quad (7)$$

$$\ln K^\circ = \frac{\Delta S^\circ}{R} - \frac{\Delta H^\circ}{RT} \quad (8)$$

where R, T and K° are the universal gas constant, temperature in Kelvin and thermodynamic equilibrium constant for the adsorption process.

The thermodynamic equilibrium constant K° can be obtained from the following equation for the distribution adsorption coefficient K_d [28]:

$$K_d = \frac{C_0 - C_e}{C_e} \cdot \frac{V}{m} \quad (9)$$

where C_0 is the initial concentration (mmol/L), C_e is the equilibrium concentration (mmol/L), V is the volume (L) of the solution and m is the sorbent weight (g). The thermodynamic equilibrium constant K° can be determined by plotting ln K_d versus C_e and extrapolating to a C_e of zero. ΔH° and ΔS° can be obtained from the slope and intercept, respectively, of the linear plot of ln K° versus $1/T$.

The thermodynamic parameters for VMP05-3, which had the highest q_m, were calculated. The value for ln K° was obtained from the intercept of the linear plot of ln K_d versus C_e, and its plot versus. $1/T$ is given in Fig. 10. The standard enthalpy and entropy changes were calculated from the slope and intercept of this plot. The thermodynamic parameters calculated from Eqs. (7)–(9) are listed in Table 4. The negative values of standard Gibbs free energy at the different temperatures indicate spontaneous processes and the decrease in the values of ΔG° with increasing temperature reveals that the adsorption process was less favorable at higher temperatures. The negative enthalpy change (ΔH°) shows that the adsorption of indium ion onto the synthesized microbeads is an exothermic process. The values for ΔH° being between 40 and 120 kJ/mol indicated chemisorption, which has higher values than physisorption [31], and thus these values reveal that the adsorption is chemisorption. The negative entropy change (ΔS°) reflects the decreasing randomness at the solid/liquid interface during the adsorption process.

3.9. Effect of pH on indium adsorption

The pH of the aqueous solution is an important parameter in the adsorption process. The influence of pH on the indium adsorption of VMP05-3 was investigated by varying the pH, and the results are given in Fig. 11. The amount of indium adsorbed per gram of microbeads increased rapidly as the pH increased to a pH of 6 and thereafter remained approximately 0.7 mmol/g. The decrease in the amount of indium adsorbed at lower pH values ($\leq$6.0) resulted from the higher concentration of H^+ ions competing with the In^{3+} ions

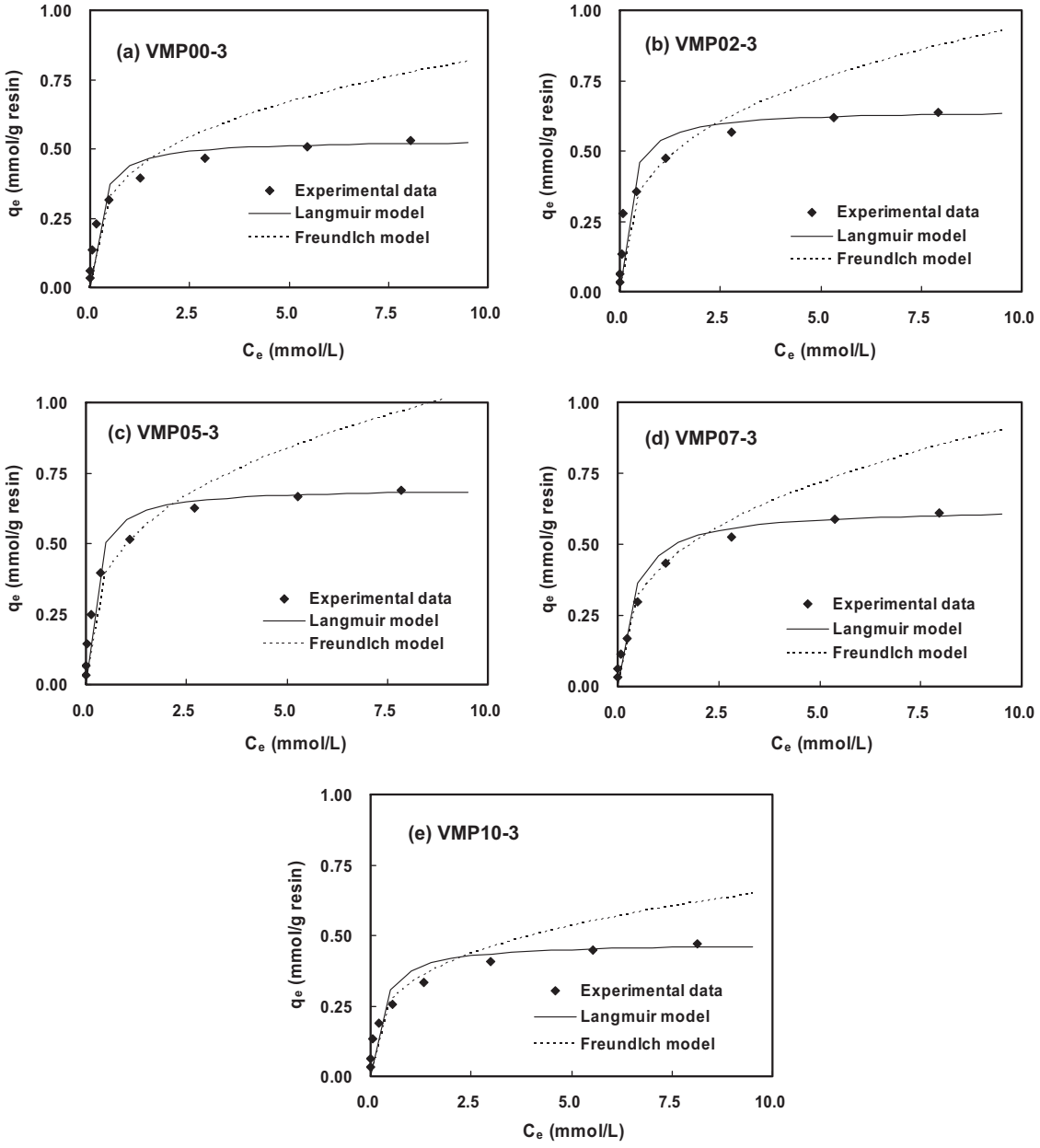

Fig. 9. Adsorption isotherms for indium onto the microbeads.

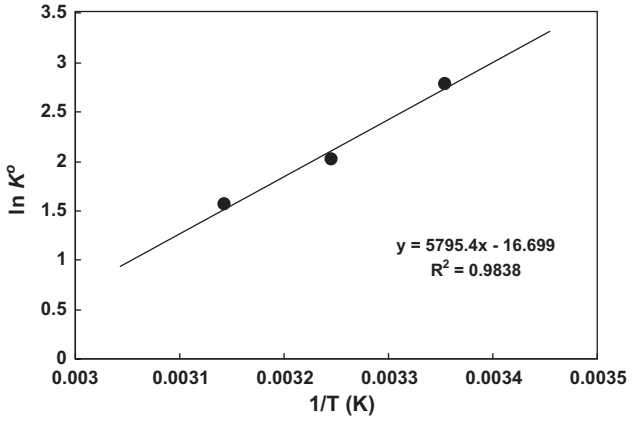

Fig. 10. Linear plot of ln K° versus $1/T$ for the adsorption of indium onto VMP05-3 at 298.15, 308.15 and 318.15 K.

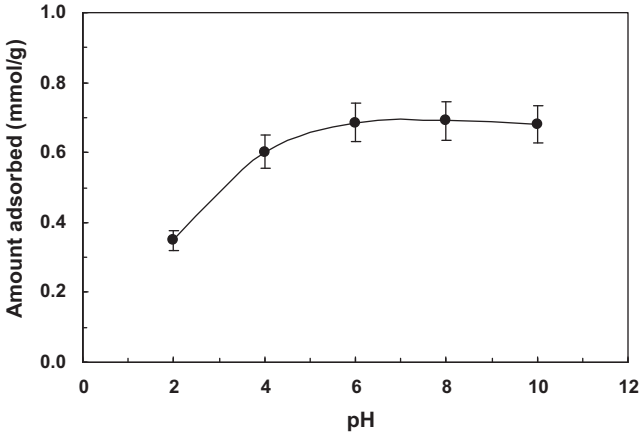

Fig. 11. The effect of pH on indium adsorption onto the microbeads.

for the adsorption sites of the microbeads. In contrast, the indium adsorption was constant at higher pH values (≥6.0) because the In^{3+} ions were not competing with H^+ ions due to their lower concentrations [32].

4. Conclusions

Microbeads were synthesized by suspension polymerization using 5 monomer ratios and 3 crosslinking-agent concentrations, and their adsorption properties were investigated. The structures of the microbeads were confirmed by FT-IR, and the size of the microbeads was confirmed to be 100–200 μm by SEM analysis. The synthetic yields decreased with increasing VPA content resulting from a lower conversion of VPA than for the other monomers as determined by EDS analysis.

TGA analysis confirmed that the functional groups —COOH and $-PO_3H_2$, which are responsible for the ion-exchange capability of the microbeads, are thermally stable at temperatures up to 260 °C; the crosslinking structure was destroyed at temperatures above 400 °C. Therefore, the microbeads synthesized in this study are suitable for use in applications at temperatures up to 260 °C.

The water uptake was proportional to the VPA content, and the IEC was inversely proportional to the VPA content. However, the amount of indium adsorbed was highest at a 50% mole ratio of VPA because of the conversion of VPA and the synthetic yields. Moreover, the water uptake and IEC were superior at lower concentrations of crosslinking agent. However, the microbeads did not form with a crosslinking-agent concentration of 20 wt%. We determined that the optimum conditions for the preparation of the microbeads were 30 wt% crosslinking agent and a 5:5 mol ratio of the monomers.

Under the optimum conditions, the adsorption capacity of indium was 0.70 mmol/g resin, the water uptake was 101% and the synthetic yield was 75%. The thermodynamic parameters (ΔG°, ΔH° and ΔS°) were calculated from the temperature dependent adsorption isotherms and indicate that the adsorption was spontaneous and endothermic.

Acknowledgements

This research was supported by the Pioneer Research Center Program through the National Research Foundation of Korea, which is funded by the Ministry of Education, Science and Technology (grant number 2011-0001667/20110001671), and by the Ministry of Education, Science and Technology (MEST) and the National Research Foundation of Korea (NRF) through the Human Resource Training Project for Regional Innovation (no. I00087).

References

[1] S.-J. Hsieh, C.-C. Chen, W.C. Say, Process for recovery of indium from ITO scraps and metallurgic microstructures, Mater. Sci. Eng. B: Adv. 158 (2009) 82–87.
[2] H.-M. Liu, C.-C. Wu, Y.-H. Lin, C.-K. Chiang, Recovery of indium from etching wastewater using supercritical carbon dioxide extraction, J. Hazard. Mater. 172 (2009) 744–748.
[3] W.-L. Chou, C.-T. Wang, K.-Y. Huang, Effect of operating parameters on indium (III) ion removal by iron electrocoagulation and evaluation of specific energy consumption, J. Hazard. Mater. 167 (2009) 467–474.
[4] B. Gupta, A. Deep, P. Malik, Liquid–liquid extraction and recovery of indium using Cyanex 923, Anal. Chim. Acta 513 (2004) 463–471.
[5] H. Minamisawa, K. Murashima, M. Minamisawa, N. Arai, T. Okutani, Determination of indium by graphite furnace atomic absorption spectrometry after coprecipitation with chitosan, Anal. Sci. 19 (2003) 401–404.
[6] M. Tuzen, M. Soylak, A solid phase extraction procedure for indium prior to its graphite furnace atomic absorption spectrometric determination, J. Hazard. Mater. 129 (2006) 179–185.
[7] I.M.M. Kenawy, M.A.H. Hafez, S.A. Elwaness, Preconcentration and separation by electrodeposition of indium from its different solution complexes, Bull. Soc. Chim. Fr. 5 (1991) 677–683.
[8] L. Medvecky, J. Briancin, Possibilities of simultaneous determination of indium and gallium in binary InGa alloys by anodic stripping voltammetry in acetate buffer, Chem. Pap. Chem. Zvesti. 58 (2004) 93–100.
[9] M.C.B. Fortes, A.H. Martins, J.S. Benedetto, Indium adsorption onto ion exchange resins, Miner. Eng. 16 (2003) 659–663.
[10] F.D. Mendes, A.H. Martins, Selective sorption of nickel and cobalt from sulphate solutions using chelating resins, Int. J. Miner. Process. 74 (2004) 359–371.
[11] P.J. Dowding, B. Vincent, Suspension polymerization to form polymer beads, Colloid Surf. A 161 (2000) 259–269.
[12] Z.H. Lin, C.J. Guan, X.L. Feng, C.X. Zhao, Synthesis of macroreticular *p*-((-sulfonic-perfluoroalkylated)polystyrene ion-exchange resin and its application as solid acid catalyst, J. Mol. Catal. A: Chem. 247 (2006) 19–26.
[13] F.M.B. Coutinho, D.L. Carvalho, M.L.L.T. Aponte, C.C.R. Barbosa, Pellicular ion exchange resins based on divinylbenzene and 2-vinylpyridine, Polymer 42 (2001) 43–48.
[14] K.S. Shin, E.M. Choi, T.S. Hwang, Preparation and characterization of ion-exchange membrane using Sty/HEA/LMA terpolymer via post-sulfonation, Desalination 263 (2010) 151–158.
[15] Z. Wang, H. Ni, M. Zhang, C. Zhao, H. Na, Preparation and characterization of sulfonated poly(arlyene ether ketone sulfone)s for ion exchange membranes, Desalination 242 (2009) 236–244.
[16] T.R. Dulski, A Manual for the Chemical Analysis of Metals, ASTM International, USA, 1996.
[17] A. Tuncel, Suspension polymerization of poly(ethylene glycol) methacrylate: a route for swellable spherical gel beads with controlled hydrophilicity and functionality, Colloid Polym. Sci. 278 (2000) 1126–1138.
[18] R.M. Silverstein, F.X. Webster, D.J. Kiemle, Spectrometric Identification of Organic Compounds, John Wiley & Sons Inc., USA, 2005.
[19] Y. Yuan, J. Liu, B. Zhou, S. Yao, H. Li, W. Xu, Synthesis of coated solvent impregnated resin for the adsorption of indium (III), Hydrometallugry 101 (2010) 148–155.
[20] R. Arshady, A. Ledwith, Suspension polymerisation and its application to the preparation of polymer supports, React. Polym. Ion Exch. Sorbents 1 (1983) 159–174.
[21] W. Lin, L.T. Biegler, A.M. Jacobson, Modeling and optimization of a seeded suspension polymerization process, Chem. Eng. Sci. 65 (2010) 4350–4362.
[22] E. Uguzdogan, E.B. Denkbas, E. Ozturk, S.A. Tuncel, O.S. Kabasakal, Preparation and characterization of polyethyleneglycolmethacrylate (PEGMA)-co-vinylimidazole (VI) microspheres to use in heavy metal removal, J. Hazard. Mater. 162 (2009) 1073–1080.
[23] R. Jain, V.K. Gupta, S. Silkarwar, Adsorption and desorption studies on hazardous dye Naphtol Yellow S, J. Hazard. Mater. 182 (2010) 749–756.
[24] V.K. Gupta, B. Gupta, A. Rastogi, S. Agarwal, A. Nayak, A comparative investigation on adsorption performances of mesoporous activated carbon prepared from waste rubber tire and activated carbon for a hazardous azo dye-Acid Blue 113, J. Hazard. Mater. 186 (2011) 891–901.
[25] D. Bozic, V. Stankovic, M. Gorgievski, G. Bogdanovic, R. Kovacevic, Adsorption of heavy metal ions by sawdust of deciduous trees, J. Hazard. Mater. 171 (2009) 684–692.
[26] B.B. Sahu, K. Parida, Cation exchange and sorption properties of crystalline α-titanium(IV) phosphate, J. Colloid Interface Sci. 248 (2002) 221–230.
[27] K. Jia, B. Pan, Q. Zhang, W. Zhang, P. Jiang, C. Hong, B. Pan, Q. Zhang, Adsorption of Pb^{2+}, Zn^{2+}, and Cd^{2+} from waters by amorphous titanium phosphate, J. Colloid Interface Sci. 318 (2008) 160–166.
[28] G. Zhao, J. Li, X. Wang, Kinetic and thermodynamic study of 1-naphtol adsorption from aqueous solution to sulfonated graphene nanosheets, Chem. Eng. J. 173 (2011) 185–190.
[29] S. Hong, C. Wen, J. He, F. Gan, Y.-S. Ho, Adsorption thermodynamics of Methylene Blue onto bentonite, J. Hazard. Mater. 167 (2009) 630–633.
[30] W.S.W. Ngah, M.A.K.M. Hanafiah, Adsorption of copper on rubber (Hevea brasiliensis) leaf powder: kinetic, equilibrium and thermodynamic studies, Biochem. Eng. J. 39 (2008) 521–530.
[31] M. Alkan, O. Demirbas, S. Celikcapa, M. Dogan, Sorption of acid red 57 from aqueous solution onto sepiolite, J. Hazard. Mater. B116 (2004) 135–145.
[32] S.S. Shukla, L.J. Yu, K.L. Dorris, A. Shukla, Removal of nickel from aqueous solutions by sawdust, J. Hazard. Mater. B121 (2005) 243–246.